ARTICLE

N-methyl-2-hydroxyethylammonium oleate ionic liquid performance as corrosion inhibitor for mild steel in hydrochloric acid medium

Tobias E. Schmitzhaus[1,2] (iD) | Maria R. Ortega Vega[1] | Roberto Schroeder[1,3] | Iduvirges L. Muller[1] | Silvana Mattedi[4] | Célia de Fraga Malfatti[1]

[1]Department of Metallurgy, Laboratório de Pesquisa em Corrosão (LAPEC), Universidade Federal do Rio Grande do Sul (UFRGS), Porto Alegre, Rio Grande do Sul, Brazil

[2]Department of Metallurgy, Instituto Federal de Mato Grosso do Sul, Corumbá, Brazil

[3]Department of Mechanical Engineering, Pontifícia Universidade Católica do Rio Grande do Sul, Porto Alegre, Rio Grande do Sul, Brazil

[4]Department of Chemical Engineering, Laboratório de Termodinâmica Aplicada, Universidade Federal da Bahia (UFBA), Salvador, Bahia, Brazil

Correspondence
Tobias E. Schmitzhaus, Department of Metallurgy, Laboratório de Pesquisa em Corrosão (LAPEC), Universidade Federal do Rio Grande do Sul (UFRGS), Avenida Bento Goncalves 9500, Porto Alegre, RS 91501-970, Brazil and Department of Metallurgy, Instituto Federal de Mato Grosso do Sul, Pedro de Medeiros street, s/n, Corumbá, CEP 79310-110, Brazil.
Email: tobiasschmitzhaus@gmail.com and tobias.schmitzhaus@ifms.edu.br

Abstract

The aim of the present study is to evaluate the performance of *N*-methyl-2-hydroxyethylammonium oleate ([m-2HEA][Ol]) as a corrosion inhibitor for mild steel in a 0.1-mol/L hydrochloric acid solution and also investigate the role of chloride in the inhibition mechanism. This protic ionic liquid (PIL) has formerly shown a high efficiency as a corrosion inhibitor in a neutral chloride medium. Electrochemical and weight loss measurements, surface contact angle determination, scanning electron microscopy, and Raman spectroscopy were used to understand the factors that influence the response of the studied inhibitor. Results revealed that [m-2HEA][Ol] behaves as a mixed-type adsorption inhibitor, by blocking cathodic sites and by modifying the activation energy of the anodic reaction, and it can reach up to 94–97% of inhibition efficiency. PIL adsorption was enhanced by the excess of positive charge of the mild steel. The effect of inhibitor molecule has been discussed to propose a mechanism that explains the inhibitory action of the corrosion inhibitor, pointing out the role of chloride in the inhibition mechanism.

KEYWORDS

acid inhibitors, chemisorption, corrosion inhibitor, hydrochloric acid, mild steel

1 | INTRODUCTION

For decades, steel has been used throughout the world as a structural material in applications such as tanks, heat exchangers, distillation towers, and pipelines, which in some cases can be exposed to acidic environments.[1–4] In contact with those acidic media, steel can suffer severe damage by corrosion processes, which leads to critical failures and affects the service life of facilities and devices. The use of corrosion inhibitors has been a smart strategy, widely employed in the industry, to enhance steel corrosion resistance. The most common inhibitors used are silicates (for potable water), nitrates (for recirculating cooling waters), varieties of amines, pyridine, and quinolone (for acid applications).[5] A corrosion inhibitor is a substance capable of retarding or mitigating corrosion reactions[6] when added to the electrolyte. Organic inhibitors work out by adsorption on the metal surface, either by physisorption or chemisorption.[1–4] These mechanisms depend on the nature of the inhibitor molecule, presence of functional groups, charge density at the donor atom, molecular structure, and pH.[7]

However, some organic corrosion inhibitors are reported as being toxic to living beings or to the environment[8,9] by exposition during application and employment, synthesis,[10] accidental spill or leakage, or disposal. For this reason, there is an increasing trend toward the development of new substances that are less aggressive to the environment. As an alternative, ionic liquids (ILs) can be promising, due to their low volatility at atmospheric pressure, which ensures the absence of toxic gas emissions.[11,12]

Protic ionic liquids (PILs) comprehend a huge class of organic salts, composed of organic cations and anions with at least one motile proton, which promotes the formation of hydrogen bonds.[13–15] These structures yield the set of PIL properties, including low vapor pressure, being in the liquid phase at temperatures lower than 100°C and close to room temperature, wide *liquidus* range, high ionic conductivity, the solubility of diverse solutes and miscibility/immiscibility with a wide range of solvents,[16] relatively wide electrochemical window, and no combustibility.[11,13,17,18] PILs are thermally and chemically stable, so they can be recycled, which can make synthetic routes less expensive, more efficient, and environmentally less hazardous.[19,20] Due to all this versatility, PILs can be used in a wide range of applications such as an inert electrolyte to verify diffusivity

of protective coatings,[21] lubricants,[22–24] nonaqueous plating systems,[25] catalysis,[26] fuel cells, batteries,[27] storage media for toxic gases,[28] performance additives in pigments,[29] and corrosion inhibitors.[7,30] In consequence, they have gained attention from many industries.[27,31,32]

The use of PILs as corrosion inhibitors is very promising, owing to their potentiality to be tailored for this application by modifying their structure.[23,33] It is vital to understand how structure makes them function as corrosion inhibitors. Compounds containing functional groups such as amines and carboxylic acids were investigated by Yoo et al.,[12] Amin et al.,[34] and Amin and Ibrahim,[35] and they were reported to present promising anticorrosion effects. Tawfik[8] tested gemini cationic surfactants as corrosion inhibitors for steel in a hydrochloric acid solution and found that they behaved as a mixed-type corrosion inhibitor, by blocking mechanism on the anodic and cathodic sites, reaching 93% inhibition efficiency. Olivares-Xometl et al.[4] used 1,2-dimethyl-3-decylimidazole iodide, N-triethyl methylammonium acetate, and N-triethyl methylammonium laurate ILs as corrosion inhibitors for steel in sulfuric acid and hydrochloric acid solution, which worked as mixed inhibitors in both media.

In previous studies performed by our research group, Ortega Vega et al.[23] reported the use of N-methyl-2-hydroxyethylammonium oleate ([m-2HEA] [Ol]) and other similar ILs as lubricants for aluminum. Furthermore, Schmitzhaus et al.[36] reported in an early study that [m-2HEA][Ol] worked as mixed-type corrosion inhibitor, with predominance in anodic processes, for steel in a neutral chlorinated solution. The PILs maintained their performance even in high turbulence hydrodynamic conditions and promoted hydrophobicity on the substrate, and their adsorption was possible due to the presence of amino and carboxylic functional groups.

As, up to now, there are no reports about the use of [m-2HEA][Ol] as corrosion inhibitor for steel in acidic media, the purpose of this study was to evaluate [m-2HEA][Ol] PIL as a corrosion inhibitor for mild steel in a 0.1-mol/L hydrochloric acid solution and to verify the role of chloride in the inhibition mechanism. This study employed several techniques, such as electrochemical and weight loss measurements, surface contact angle measurement, scanning electron microscopy (SEM), and Raman spectroscopy. Results allowed evaluating the inhibition efficiency and proposing an inhibition mechanism.

TABLE 1 Steel composition of the used steel in all measurements

Element	C	Si	Mn	P	S	Cr	Al	B
wt%	0.03	0.008	0.23	0.014	0.005	0.007	0.03	0.0006

2 | EXPERIMENTAL SECTION

2.1 | Materials and samples preparation

Mild steel disc specimens with dimensions of 27 mm (diameter) × 1.4 mm (thickness), with the composition shown in Table 1, were used as a substrate.

Before all measurements, the electrodes were sanded with SiC paper from 80 grit to 1,200 grit. 3M™ tape was used to leave a test area of 2.83 cm². A copper wire was used as an electric contact. Then, samples were degreased in a neutral soap solution, washed with acetone, alcohol, and deionized water, and dried with fresh air.

To ensure the reproducibility of the tests, all measurements were performed at least in triplicates.

N-methyl-2-hydroxyethylamine was obtained from Aldrich, with 99% purity by mass, whereas oleic acid was obtained from Sigma, with purity greater than 99.5% by mass. These components were used as received. The same steps of preparation were followed for ammonium carboxylates ILs as described elsewhere.[37] In this study, the same batch of IL prepared before[23] was used and a similar chemical characterization was performed (Fourier-transform infrared spectroscopy and nuclear magnetic resonance spectroscopy) as in a previously published study.[23] The molar weight of [m-2HEA][Ol] is 357.57 g/mol, the water content of pure IL is 7.16%, its viscosity is 1,600 mPa·s, and the PIL is non-Newtonian. The [m-2HEA][Ol] is thermally stable until 200°C. The density is in the range of 0.93–0.96 g/cm³.[23,37]

For all the experiments, a freshly prepared 0.1-mol/L hydrochloric acid (Synth® 37%) solution was used. Concentrations of [m-2HEA][Ol] ranging from 0.5 to 2.5 mmol/L were tested. The pH of all prepared solutions remained at 1.60, even in the presence of [m-2HEA][Ol]. Table 2 shows the molecular structure of the PIL. The use of this PIL as a corrosion inhibitor is subject to the patent process BR 10 2019 015605-8.

2.2 | Electrochemical measurements

The electrochemical measurements were carried out exposing the steel specimens to a naturally aerated 0.1-mol/L hydrochloric acid solution, in the absence or presence of various concentrations of [m-2HEA][Ol] at 25 ± 1°C, after 30 min of immersion to reach a steady state. The experiments were performed in a conventional three-electrode cell with the mild steel working electrode, a saturated calomel reference electrode (SCE), and a platinum wire counter electrode, using an Autolab PGSTST302N potentiostat/galvanostat.

Potentiodynamic polarization tests were performed first from E_{OCP} in the cathodic direction down to −250 mV versus E_{OCP}, to avoid the influence of pre-existing oxide layers. Then samples were left at open-circuit potential (OCP) until stabilization (∼600 s). Then, the potential was scanned from E_{OCP} in the anodic direction up to +250 mV versus E_{OCP}, with a scan rate of 1.0 mV/s. Data were recorded and analyzed by NOVA 2.1.4 software.[38,39] Linear segments of anodic and cathodic curves were fitted by Tafel extrapolation to obtain corrosion current densities (i_{corr}) and corrosion rates (CRs), following ASTM G102-89 (2015).[40]

The inhibition efficiency percentage ($\eta\%$) was calculated using the following equation:

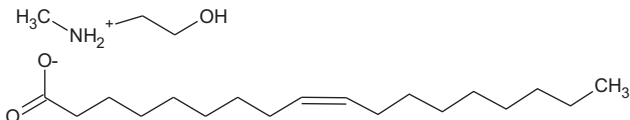$$\eta\% = \frac{i_{corr}^0 - i_{corr}^i}{i_{corr}^0} \times 100, \qquad (1)$$

where i_{corr}^0 and i_{corr}^i are the values of corrosion current density in the absence and presence of inhibitor, respectively.

The surface charge of the steel can be determined by comparing the corrosion potential (E_{corr}) with respect to the zero charge potential (E_{ZCP}).[41,42] This information helps in determining the type of adsorption that occurs on the electrode surface.[43] The surface charge of steel can be calculated by the following equation:

$$E_r = E_{corr} - E_{ZCP}, \qquad (2)$$

where E_r is Antropov's "rational" corrosion potential.[41,44] When E_r is negative, the net charge of the surface is negative, and thus the adsorption of cations is favored. However, a positive E_r means that the surface charge is positive, and then preferential adsorption of anions is expected.[45] Moreover, when the E_{ZCP} and E_{corr} are close to each other, neutral organic molecules adsorption on the metal surface is favored.[5]

TABLE 2 Structures of the studied protic ionic liquid (PIL)[23]

PIL	Structure
[m-2HEA][Ol] N-methyl-2-hydroxyethylammonium oleate	

Zero charge potential (ZCP) was determined via electrochemical impedance spectroscopy (EIS) using the method reported elsewhere.[41,42,46] Measurements were carried out using AC signals of 5 mV peak to peak in the frequency range of 10^3–10^2 Hz and by applying different potentials, with and without [m-2HEA][Ol]. This frequency range was used, because at enough high frequencies, the electrical double-layer capacitor shortcuts the Faradaic reactions.[43] C_{dl} was calculated from the following equation[43]:

$$C_{dl} = Y_0(\omega_{max})^{n-1}, \tag{3}$$

where $\omega_{max} = 2\pi f_{max}$, and f_{max} is the frequency at which the imaginary component of the impedance is maximal. The potential corresponding to the minimum value of C_{dl} is considered as the ZCP of the electrode.[42,43,47]

Chronoamperometry tests were performed by polarizing the steel electrode to −700 and −485 mV (vs. SCE) for 1 hr. Initially, the steel electrode was polarized in the blank solution for 10 min to initiate corrosion. Thereafter, IL was added to evaluate the behavior of the system.[48,49]

2.3 | Weight loss measurements

Weight loss measurements were carried out taking ASTM G31-72 (2004)[50] as a reference, with an adaptation in the cleansing procedure. A laboratory oven (FANEM model 315 SE) and Evolution MT-512E 2HP temperature controller were used to guarantee 25°C. The solution volume was 500 ml, and the mild steel specimens with 6.7 cm² of the exposed area were immersed in a 0.1-mol/L hydrochloric acid solution for 120 hr (5 days), with and without [m-2HEA][Ol] corrosion inhibitor. At the end of the test, specimens were removed, carefully washed with deionized water, dried with cold air, and then weighed on a Shimadzu AY220 analytical balance. CR was obtained by the following equation:

$$CR = \frac{K \times W}{A \times t \times D}, \tag{4}$$

where K is a constant (8.76×10^4 for mm/year), W is the mass loss in g, A is the area in cm², t is the time in hr, and D is the density of steel (7.874 g/cm³). The inhibition efficiency ($\eta\%$) was calculated from the weight loss data according to the following equation[50,51]:

$$\eta\% = \left(1 - \frac{W}{W_0}\right) \times 100. \tag{5}$$

2.4 | Surface analysis

The surface morphology of steel specimens after weight loss tests (5 days) was examined by an SEM Hitachi TM3000 Tabletop Microscope. Bruker ContourGT-K Optical interferometer (green light) was used to evaluate surface topography and to obtain the Sz parameter, which is the 10-point height over the complete three-dimensional (3D) surface.

A homemade goniometer was used to perform contact angle measurements on the steel surface using a 0.7-μl drop of water. Before the test, plates were immersed in the different electrolytes for 1 hr. After immersion, samples were cleaned with deionized water and dried with fresh air. Pictures of the drop were taken with a computer-controlled camera; the angles were computed using Surftens 4.5 software. Contact angle values correspond to the average of five records.

Raman spectra were obtained using Renishaw inVia Spectrometer to evaluate the metal–organic interaction after weight loss measurements.

3 | RESULTS AND DISCUSSION

3.1 | Contact angle measurements

The water contact angle of the steel surface after immersion in the inhibited and uninhibited solution was measured to evaluate PIL adsorption on the surface. From Figure 1, it is observed that the water contact angles on steel increased with the increase of PIL concentration in the following order: steel in 0.1-mol/L hydrochloric acid (undetermined) < steel in 0.1-mol/L hydrochloric acid + 0.25-mmol/L [m-2HEA][Ol] (66°) < steel in 0.1-mol/L hydrochloric acid + 0.50-mmol/L [m-2HEA][Ol] < steel in 0.1-mol/L hydrochloric acid + 1.25-mmol/L [m-2HEA][Ol] (79°) < steel in 0.1-mol/L hydrochloric acid + 2.50-mmol/L [m-2HEA][Ol].

The low value of the contact angle on steel after immersion in an uninhibited solution (Figure 1a) reveals that the corroded steel exhibits hydrophilic behavior. It is attributed to the presence of corrosion products, which causes the spreading of the water drop on the metal surface.[52–54]

With the addition of 0.25-mmol/L [m-2HEA][Ol] into solution, the contact angle increased from close to 0 to 66°, which points out a more hydrophobic behavior.[55] This hydrophobic behavior can be explained by the presence of an adsorbed layer of [m-2HEA][Ol], which has an amphiphilic character, on the metal surface. In [m-2HEA][Ol] molecules, the carboxylate function in the anion and the cation moiety is hydrophilic, and the alkyl
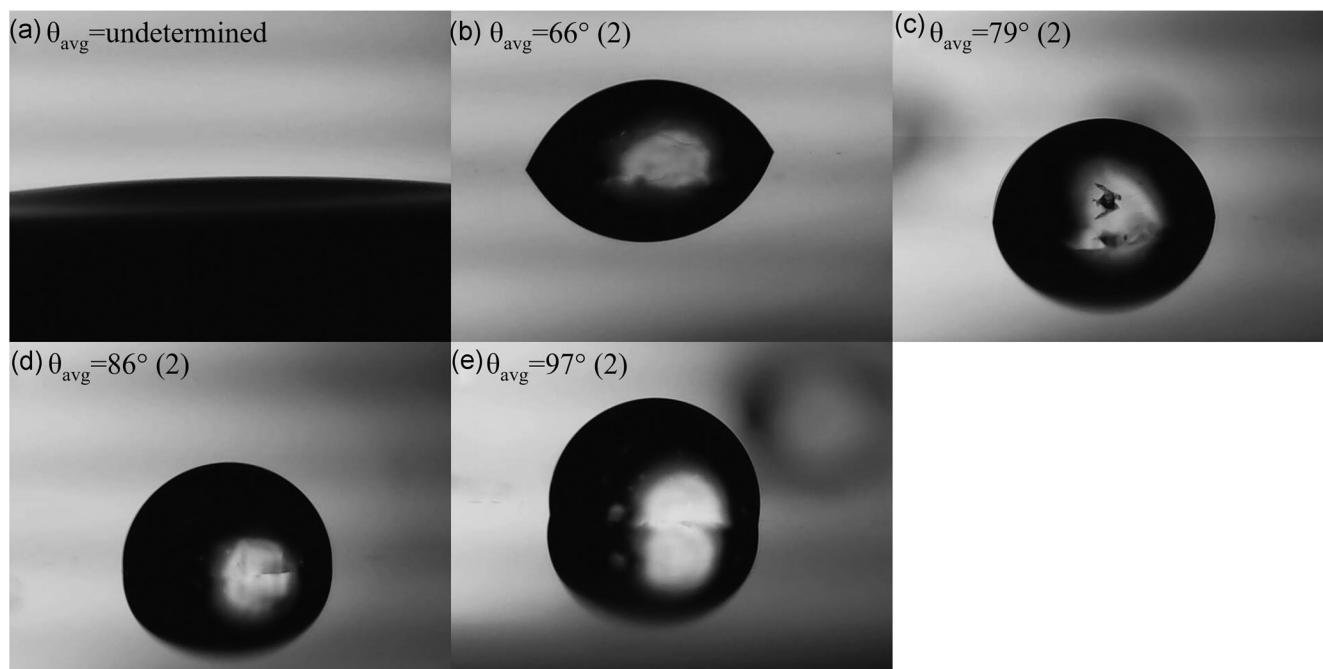
FIGURE 1 The water contact angle for steel after 1-hr immersion in corrosion solutions: (a) 0.1-mol/L hydrochloric acid; (b) 0.1-mol/L hydrochloric acid + 0.25-mmol/L *N*-methyl-2-hydroxyethylammonium oleate ([m-2HEA][Ol]); (c) 0.1-mol/L hydrochloric acid + 0.50-mmol/L [m-2HEA][Ol]; (d) 0.1-mol/L hydrochloric acid + 1.25-mmol/L [m-2HEA][Ol]; (e) 0.1-mol/L hydrochloric acid + 2.50-mmol/L [m-2HEA][Ol]. Values in parentheses are the standard deviation

chain of the anion is hydrophobic, according to Álvarez et al.[37,56] As the water contact angle increases with the increase of [m-2HEA][Ol] concentration, it can be stated that hydrophobicity of the steel surface is a function of PIL concentration. The presence of more PIL molecules on the substrate means that the surface is covered with more hydrophobic moiety, as it is more voluminous than the PIL counter ion; thus, the hydrophobic anion occupies the most of the metal surface. This result coincides with those reported by other authors.[57]

In addition, a low contact angle can also be related to less corrosion products on the metal surface. Hydrophobic behavior inherently means that it becomes harder for the electrolyte to wet the surface, which consequently hinders the interaction between corrosive agents and metallic surfaces, and thus the formation of corrosion products.[58]

3.2 | OCP measurements

OCP results for all the studied electrolytes are presented in Figure 2. In only hydrochloric acid solution, the potential stood at a virtually stable value, whereas the solution containing 2.5 mmol/L of the inhibitor presented only a slight increase of potential value, from −548 mV in a 0.1-mol/L hydrochloric acid solution to −506 mV versus SCE. The changes in the OCP values comparing systems

in the presence/absence of an inhibitor are often useful indicators of the reaction that is more affected: cathodic or anodic.[59,60] The addition of PIL to the hydrochloric acid solution shifts the OCP toward more positive values as a function of the PIL concentrations. This positive
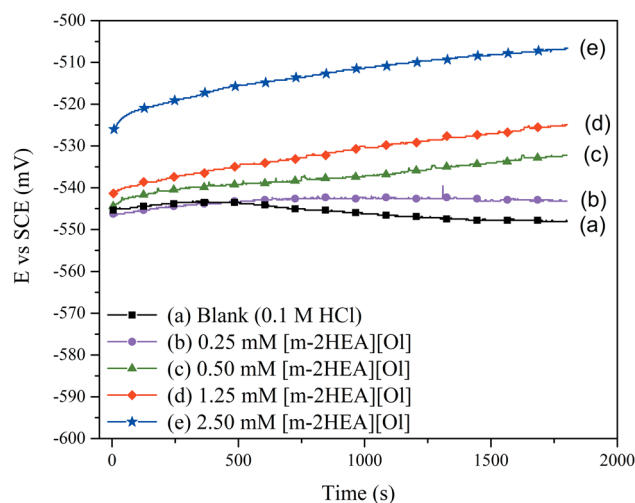

FIGURE 2 Open-circuit potential measurements for steel in a 0.1-mol/L hydrochloric acid solution in the presence and absence of *N*-methyl-2-hydroxyethylammonium oleate ([m-2HEA][Ol]) [Color figure can be viewed at wileyonlinelibrary.com]

OCP shift indicates that [m-2HEA][Ol] has the ability to inhibit the acid corrosion of steel.[61,62]

It is well accepted that the inhibition mechanism of organic corrosion inhibitors is adsorption. These types of inhibitors can affect the CR in two ways[60,63]: (a) by geometric blocking of the reaction sites (geometric blocking effect), decreasing the available reaction area, and (b) by modifying the activation energy of the cathodic and/or anodic reactions, compared with the noninhibited corrosion process. It is a difficult task to distinguish which aspects of the inhibiting effect are related to the geometric blocking action and which are related to the energy effect. Theoretically, no shifts in the corrosion potential should be observed after the addition of the corrosion inhibitor if the geometric blocking effect is stronger than the energy effect.[60,63]

3.3 | Potentiodynamic polarization measurements

Potentiodynamic polarization curves, performed at 25°C, as shown in Figure 3, provide more information about the kinetics of the processes that take place in inhibitor-free and inhibited media. Tafel extrapolation parameters, CR, and inhibition efficiency ($\eta\%$) are presented in Table 3.

From the potentiodynamic polarization curves (Figure 3) and Tafel extrapolation data (Table 3), it can be observed that E_{corr} shifts to more positive values with the increase of [m-2HEA][Ol] concentration. Concentrations between 2.5 and 0.5 mmol/L decreased the cathodic current densities to nearly the same value (in the 50 $\mu A/cm^2$ magnitude order); for the 0.25-mmol/L concentration of [m-2HEA][Ol], this decrease is less pronounced (being in the 450 $\mu A/cm^2$ magnitude order). This corrosion current diminution can be related to the surface blocking effect of the cathodic processes; as observed by the curve profile, only kinetics of the oxygen reduction reaction is affected. At concentrations lower than 0.5 mmol/L, the current reduction seems to be a function of inhibitor concentration, but at higher concentrations, the cathodic current is not affected by this variable anymore.

Cathodic Tafel slopes, β_c (presented in Table 3), did not change significantly, just a difference of 4 mV/dec (with 7 mV of standard deviation) between blank acid solution and 2.5-mmol/L [m-2HEA][Ol] solution. Generally, the hydrogen evolution reaction (HER) follows one of two very common mechanisms: Volmer–Heyrovsky or Volmer–Tafel. Both mechanisms consider several steps at different rates and also consider adsorption of a hydrogen atom on a metal surface (MH_{ads}) before H_2 evolution.[64] The presence of the PILs as a corrosion inhibitor in the corrosive solution may retard the formation of MH_{ads} or retard the electron transfer toward the hydronium ions.[7] Given that no changes in β_c were observed in this study, HER is diminished entirely by the

geometric blocking effect of [m-2HEA][Ol], which could be enhanced by the big size of the PIL molecule.[60,63,65]

Regarding the anodic region of the polarization curves, the anodic currents decrease with the increase of the inhibitor concentration. A solution containing 0.25-mmol/L [m-2HEA][Ol] presents a lower current density, compared with the uninhibited acid, and β_a suffers a slight diminution, that is, for this lowest concentration, [m-2HEA][Ol] acts only by the surface blocking effect. At concentrations between 0.5- and 2.5-mmol/L [m-2HEA][Ol], anodic Tafel slopes (Table 3) decrease down to values of 39–40 mV/dec, compared with 54 mV/dec of the inhibitor-free electrolyte, which could be related to a change in the anodic reaction mechanism (iron dissolution). The adsorbed inhibitor modifies the way that corrosion products are formed or even modifies the kind of corrosion product, and the electrode processes can then follow alternative steps through intermediates containing the inhibitor.[63] In addition, the lowering of the anodic Tafel slope could mean that the lower activation energy effect opposes the inhibition effect caused by the geometric blocking of the surface; in other words, the inhibitor molecule depolarizes anodic dissolution reaction, but the geometric blocking effect prevails.[60] This depolarization could be due to the increase of negative ions' adsorption, caused by anionic adsorption of the COO^- group present in the PIL, which lowers the overpotential of anodic reaction, that is, the increase in the adsorption of negative ions facilitates the dissolution of steel.[66] i_{corr} values (Table 3) decreased from 106 to 6.73 $\mu A/cm^2$ according to the inhibitor concentration, and η(%), as expected, increased up to 94% in the
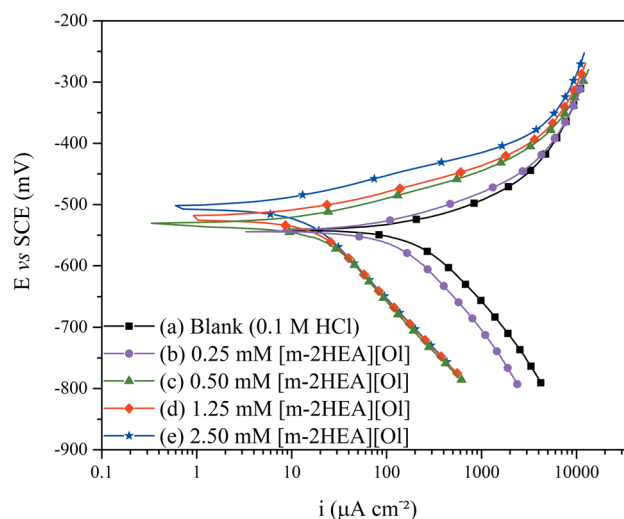

FIGURE 3 Polarization curves of steel in a 0.1-mol/L hydrochloric acid solution in the absence and presence of different concentrations of the protic ionic liquid ([m-2HEA][Ol]) at 25°C. [m-2HEA][OI], N-methyl-2-hydroxyethylammonium oleate [Color figure can be viewed at wileyonlinelibrary.com]

TABLE 3 Potentiodynamic polarization parameters for mild steel in the absence and presence of the [m-2HEA][Ol] protic ionic liquid as a corrosion inhibitor

	E_{corr} (mV vs. SCE)	i_{corr} ($\mu A/cm^2$)	CR (mm/year)	β_a (mV/dec)	β_c (mV/dec)	η (%)
0.1 mol/L HCl	−546 (3)	106 (13)	1.23	54 (4)	84 (10)	–
0.25 mmol/L [m-2HEA][Ol]	−544 (2)	64 (3)	0.74	47 (1)	96 (9)	39.7
0.50 mmol/L [m-2HEA][Ol]	−524 (4)	12 (4)	0.14	39 (2)	84 (10)	88.4
1.25 mmol/L [m-2HEA][Ol]	−519 (2)	8 (1)	0.10	39 (1)	86 (1)	92.1
2.50 mmol/L [m-2HEA][Ol]	−501 (1)	7 (1)	0.08	40 (0)	88 (7)	93.6
0.1 mol/L H_2SO_4	−537 (5)	138 (14)	1.61	60 (1)	96 (3)	–
0.1 mol/L H_2SO_4 + 0.01 mol/L NaCl	−529 (2)	127 (15)	1.47	55 (2)	96 (2)	–
0.1 mol/L H_2SO_4 + 2.5 mmol/L [m-2HEA][Ol]	−529 (5)	66 (8)	0.73	50 (3)	120 (6)	52.1
0.1 mol/L H_2SO_4 + 0.01 mol/L NaCl + 2.5 mmol/L [m-2HEA][Ol]	−508 (1)	43 (2)	0.51	44 (2)	95 (3)	68.5

Note: Values in parenthesis is standard deviation.

Abbreviation: CR, corrosion rate; SCE, saturated calomel reference electrode; [m-2HEA][Ol], *N*-methyl-2-hydroxyethylammonium oleate.

presence of [m-2HEA][Ol]. It means that the CR can be diminished with an increase of [m-2HEA][Ol] concentration. As both anodic and cathodic currents decreased in the presence of [m-2HEA][Ol], this inhibitor may be considered as a mixed-type one. A possible mechanism would be that [m-2HEA][Ol] acts by blocking cathodic sites without interfering in the mechanism of the hydrogen production reaction and by modifying the activation energy of the anodic reaction, but retaining the geometric surface blocking effect. Table 3 also shows polarization curve data for sulfuric acid solutions, which are discussed in Section 3.10 (Figure 14).

3.4 | Weight loss measurements

Weight loss is a nonelectrochemical technique for the determination of CRs and inhibitor performance. It provides more reliable results than electrochemical techniques, as the experimental conditions are approached in a more realistic way. However, immersion tests demand solid experimental procedures and are time-consuming. Results are presented in Figure 4, and for the studied systems, the η(%) increases with the concentration increase of [m-2HEA][Ol]. The values of CR obtained from weight loss are higher than those obtained on the basis of electrochemical tests for 0.1-mol/L hydrochloric acid solution. In systems containing 0.25-mmol/L [m-2HEA][Ol], the corrosion rate calculated from electrochemical data is higher than those obtained from weight loss calculations. To clarify these differences, Figure 4 compares

the CRs for all studied systems obtained from both techniques.

In Figure 4, an important difference between CR obtained from weight loss and that obtained from the electrochemical method is noticeable, especially for the blank system. It affects directly the calculations of inhibition efficiency. These results can be explained because iron dissolution occurs not only by electrochemical but also by "chemical" mechanism, which cannot be detected by electrochemical techniques,[67] denominated as anomalous dissolution. This phenomenon has been
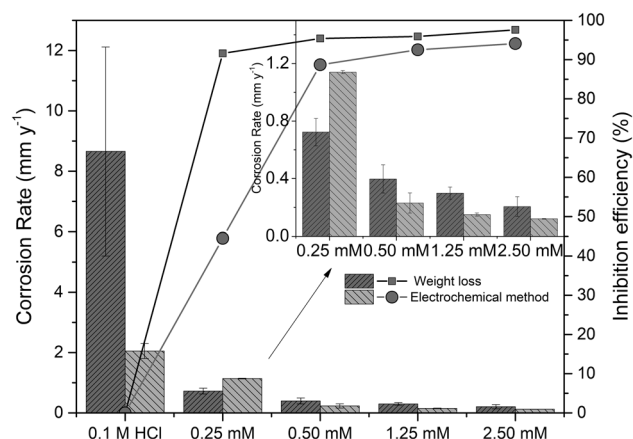

FIGURE 4 The corrosion rate and inhibition efficiency obtained by weight loss and electrochemical methods for steel in 0.1-mol/L hydrochloric acid in the absence and presence of various concentrations of *N*-methyl-2-hydroxyethylammonium oleate inhibitor

reported to occur in several metals when they are exposed to aggressive acid environments, for example, sulfuric or hydrochloric acid solutions.[68] Marsh and Schaschl[69] have shown that iron in sulfuric acid solutions of pH 2 corroded two times faster than expected from electrochemical measurements due to disintegration (i.e., chunk effect). This phenomenon was ascribed to the chemical dissolution of iron. The reaction proposed for this dissolution is represented by the following equations[67,70]:

$$Fe + H_2O \leftrightharpoons FeOH + H, \tag{6}$$

$$FeOH + H^+ \rightarrow FeOH^+ + H, \tag{7}$$

$$2H \rightarrow H_2. \tag{8}$$
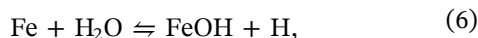
However, the "chemical" dissolution of steel, according to Equations (6)–(8), is not the only process responsible for the "anomalous" dissolution of steel. It is possible that this "anomalous" dissolution is greatly influenced by hydrogen embrittlement and the "chunk effect," that is, by the removal of small pieces of iron into the solution and their subsequent dissolution, which increases the overall amount of Fe^{2+} ions.[67,68]

Solutions containing [m-2HEA][Ol] presented smaller differences between weight loss and electrochemical method, that is, all "anomalous" phenomena are retarded due to [m-2HEA][Ol] adsorption in both cases. Therefore, electrochemical data fit in a better way with weight loss data. For these cases, the weight loss experiments added information about how iron corrodes and [m-2HEA][Ol] adsorbs, demonstrating that the inhibitor holds the effectiveness even for long times.

3.5 | Zero charge potential (E_{ZCP}) analysis

Figure 5 reveals the relationship between C_{dl} and the electrode potential from −300 to +300 mV versus E_{corr} for both blank solution and with the addition of 2.5-mmol/L [m-2HEA][Ol], determined by EIS. The potential corresponding to the minimum value of C_{dl} in plot C_{dl} versus applied potential is considered the E_{ZCP} of the electrode.[42,43] The values of E_{corr}, E_{ZCP}, and E_r are presented in Table 4.

Figure 5 shows that the double-layer capacitance value decreases 20 times with the addition of 2.5-mmol/L [m-2HEA][Ol], compared with 0.1-mol/L hydrochloric acid solution. This is due to the fact that the double layer at the metal/electrolyte interface is pushed apart by adsorption of the long-chained organic molecules, which causes a diminution of capacitance.[71–74] This general

decrease reveals that IL molecules are adsorbed on both cathodic and anodic sites. In the anodic direction, the C_{dl} increase is attributed to the adsorption of chloride ions or hydroxyl ions formed during the dissolution of steel. In the cathodic potentials, the C_{dl} increases due to H^+ adsorption.[75,76]

E_{ZCP} values (Table 3) indicate that mild steel surface carries an excess of positive charge in the absence and in presence of [m-2HEA][Ol] at OCP. These results suggest that electrostatic adsorption of chloride ions is energetically favored, which, otherwise, would take place only due to its electronegativity.[42,77,78] In consequence, due to Cl^- adsorption on the steel surface, some sites become negatively charged.[41,45]

Thus, two adsorption mechanisms can be proposed: first, the protonated part of [m-2HEA][Ol] can form an electrostatic bond with Cl^- ions earlier adsorbed on the steel surface, and PIL molecules may attach to the metal surface through chloride bridges.[44] Meanwhile, the IL anion (carboxylic function) physically adsorbs on the positively charged steel surface. It means that chloride ions act as a bridge to subsequent adsorption of [m-2HEA][Ol] on the steel surface, and then physisorption turns into chemisorption. A similar behavior was reported for different molecules on metal surfaces elsewhere,[52,71,79–81] evidencing the importance of halide ions on the adsorption mechanism. The second possible mechanism is that chemisorption could be caused by electron sharing between the IL and the vacant d-orbital of the metal, as reported by Guo et al.[52] In addition, physisorption could occur through lone electron pair
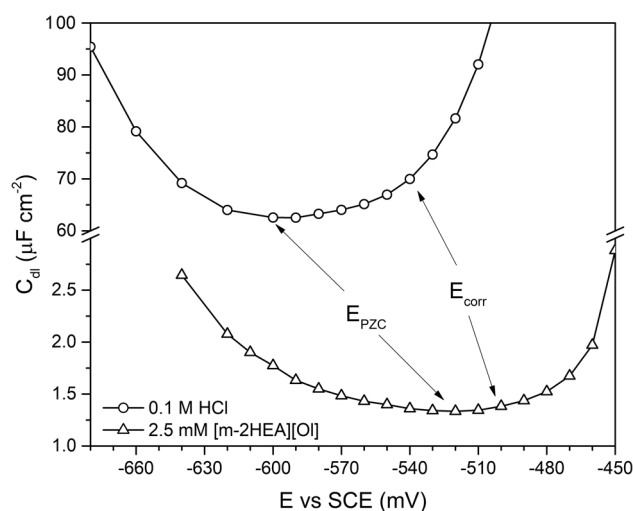
FIGURE 5 The double-layer capacitance (C_{dl}) versus applied potential (vs. SCE) on a steel plate immersed in a 0.1-mol/L HCl solution with and without N-methyl-2-hydroxyethylammonium oleate ([m-2HEA][Ol]). SCE, saturated calomel reference electrode

TABLE 4 Values of E_{corr}, E_{ZCP}, and E_r after 1 hr of immersion recorded for steel in 0.1-mol/L hydrochloric acid with and without 2.5-mmol/L [m-2HEA][Ol]

	E_{corr} (mV vs. SCE)	E_{ZCP} (mV vs. SCE)	$E_r = E_{corr} - E_{ZCP}$ (mV vs. SCE)
0.1 mol/L hydrochloric acid	−527	−590	63
0.1 mol/L hydrochloric acid + 2.5 mmol/L [m-2HEA][Ol]	−502	−523	22

Abbreviations: SCE, saturated calomel reference electrode; ZCP, zero charge potential; [m-2HEA][Ol], *N*-methyl-2-hydroxyethylammonium oleate.

donation of N and O heteroatoms to the vacant *d*-orbital of iron.[82] This whole mechanism forms a compact adsorption layer, which acts as a barrier against steel corrosion.[41,45,83,84]

3.6 | Chronoamperometric analysis

Chronoamperometry is employed to clarify how fast [m-2HEA][Ol] adsorbs on the metal surface that is already "pre-corroded."[48] For these experiments, the electrodes were polarized above or below the E_{ZCP} to determine the influence of the surface charge of the steel on the whole adsorption mechanism.

The chronoamperometric curves of 0.1-mol/L hydrochloric acid solution with an injection of 2.5-mmol/L [m-2HEA][Ol] are shown in Figure 6. Under anodic potential, the current density in the inhibitor-free solution is high, which remains nearly constant during the first 600 s (until the injection of [m-2HEA][Ol]). During the initial 100 s (before PIL injection), the decrease of current density could be ascribed to the accumulation of corrosion products at the metal/solution interface due to metal dissolution.[85]

After the injection of [m-2HEA][Ol] into solution, current density decreases at both anodic and cathodic potentials due to its direct interference in the electrochemical reactions. The current transient after injection of [m-2HEA][Ol], in anodic polarization, took 8–9 min to stabilize, and in cathodic condition, the current transient lasted for 21 min. This difference on time to stabilize the current density is caused by the surface charge: in a cathodic condition, surface should be negatively charged (below ZCP), which causes repulsion of chloride ions and interference in adsorption mechanism. However, active sites for hydrogen evolution are blocked, promoting the current value reduction. The proposed mechanism considers Cl^- as a bridge for the positive part of IL adsorption, but also the direct adsorption of the negative part of IL. In any case, both conditions converge to a high degree of coverage. The percentage of current reduction, which can also be thought of as the inhibition efficiency at each reaction (anodic iron dissolution and cathodic H_2 evolution, respectively), reaches a value of 98% for both anodic and cathodic potentials. The current values were ascribed to be a function of the occupation of active sites.[48,86] In addition, the current density after injection of the inhibitor and after the current transient remains almost constant at both −485 and −700 mV(SCE) over 1 hr. It demonstrates that [m-2HEA][Ol]
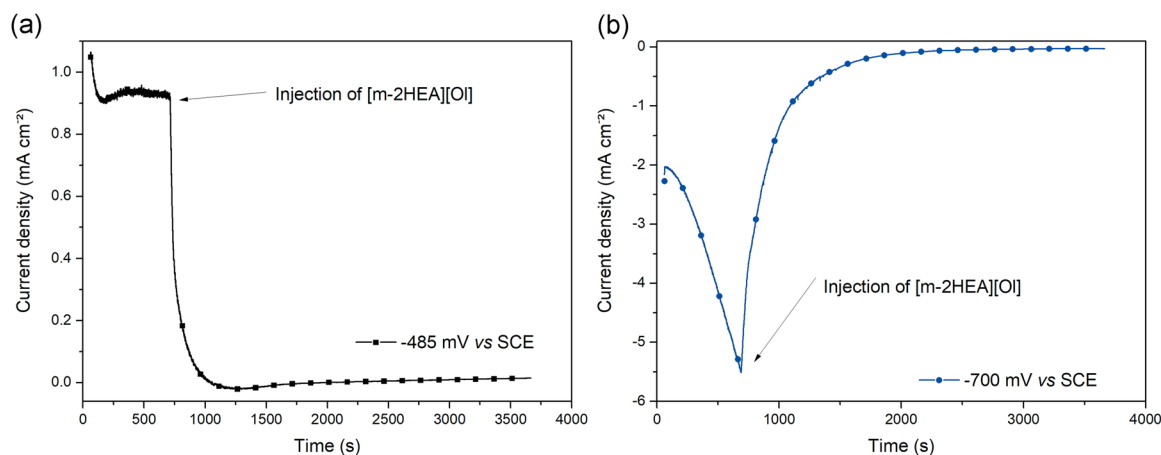

FIGURE 6 Chronoamperometric curves of steel electrodes in a 0.1-mol/L hydrochloric acid solution with an injection of 2.5 mmol/L *N*-methyl-2-hydroxyethylammonium oleate ([m-2HEA][Ol]) at (a) −485 mV versus SCE and (b) −700 mV versus SCE. SCE, saturated calomel reference electrode [Color figure can be viewed at wileyonlinelibrary.com]
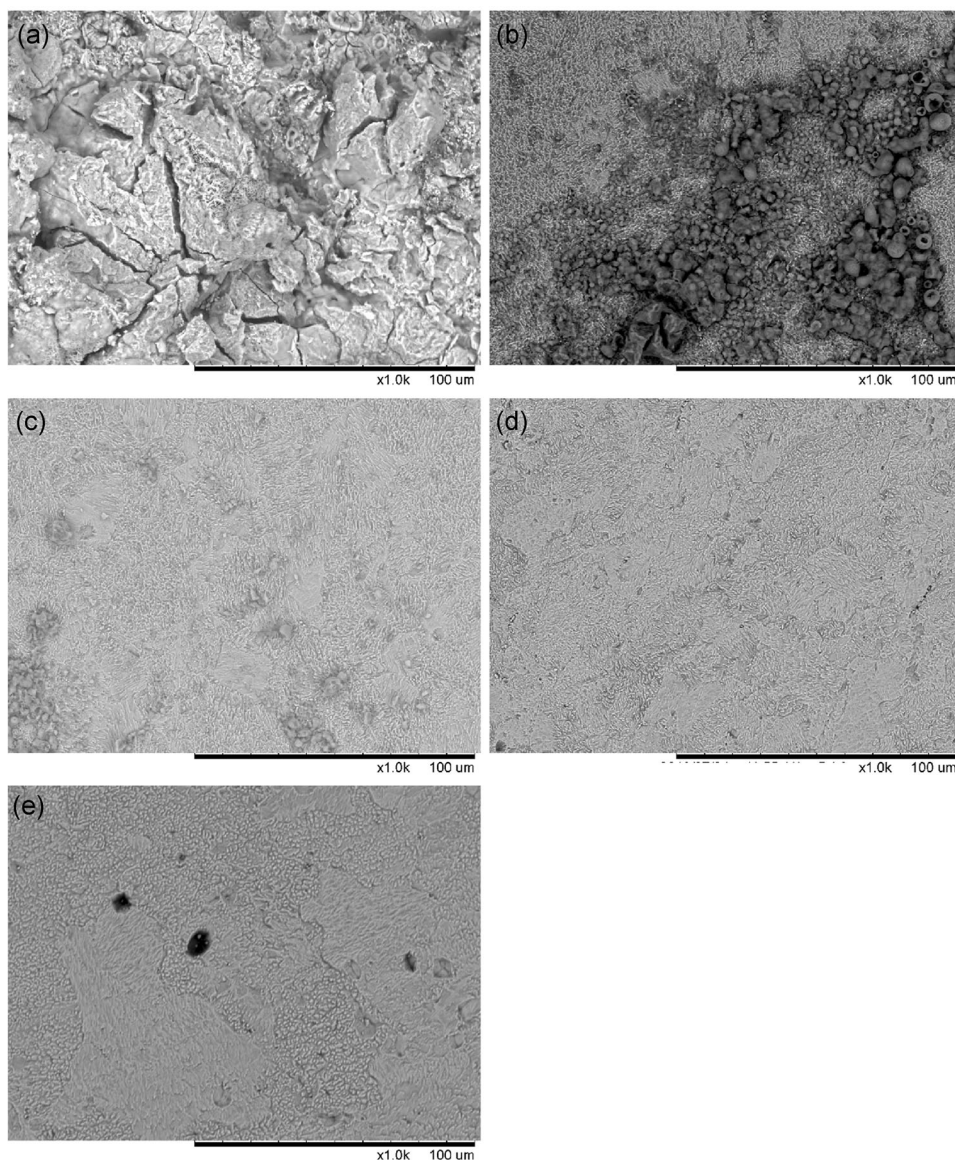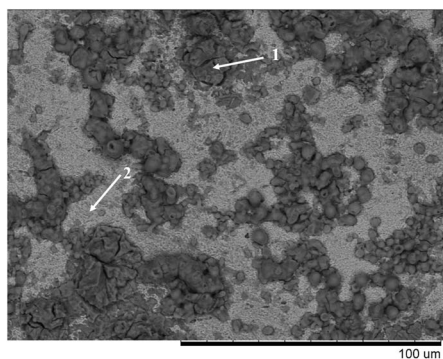
FIGURE 7 Scanning electron microscopy images of steel after 120-hr immersion in (a) 0.1-mol/L hydrochloric acid, (b) 0.25-mmol/L, (c) 0.5-mmol/L, (d) 1.25-mmol/L, and (e) 2.50-mmol/L *N*-methyl-2-hydroxyethylammonium oleate

	Fe (at.%)	C (at.%)	N (at.%)	O (at.%)	Chloride (at.%)
1	33	15	0.8	51	0.15
2	52	32	1.23	14.6	0.04

FIGURE 8 The scanning electron microscopy image and the amount of carbon, oxygen, nitrogen, chloride, and iron at different points of the steel surface after 120-hr immersion in *N*-methyl-2-hydroxyethylammonium oleate

molecules adsorb strongly on the steel surface and form a stable and protective film on the surface.[85,87]

3.7 | Surface analysis

SEM images of the steel electrode after 120 hr of immersion with and without [m-2HEA][Ol] are presented in Figure 7. Figure 7a reveals that the steel sample after 1-hr immersion in an uninhibited 0.1-mol/L hydrochloric acid solution suffers an aggressive attack of the corroding medium, with corrosion products all over the surface. Furthermore, the surface is rough. In the presence of [m-2HEA][Ol] (Figure 7b–e), the steel surface presents less corrosion marks and a different morphological aspect, resembling hives. There are regions with texturized appearance, caused

by the PIL adsorption. This molecule was reported before by Alvarez et al.[13,56] as having the property of forming supramolecular aggregates such as micelles. Figure 7d–e, referring to concentrations of 0.5-, 1.25-, and 2.5-mmol/L [m-2HEA][Ol], present a decreasing amount of corrosion products, but still present the same "texture." In 1.25- and 2.50-mmol/L [m-2HEA][Ol] solutions, steel showed less corrosion marks, due to the presence of the PIL protective layer confirmed by energy-dispersive X-ray spectroscopy (EDX) analysis.

SEM/EDX images (Figure 8) of samples immersed in a 0.25-mmol/L [m-2HEA][Ol] solution reveal that carbon and nitrogen are present all over the surface, even in corrosion products. This indicates that both parts of IL (cation and anion) are present in the protective layer. Depending on the inhibitor concentration, it did not
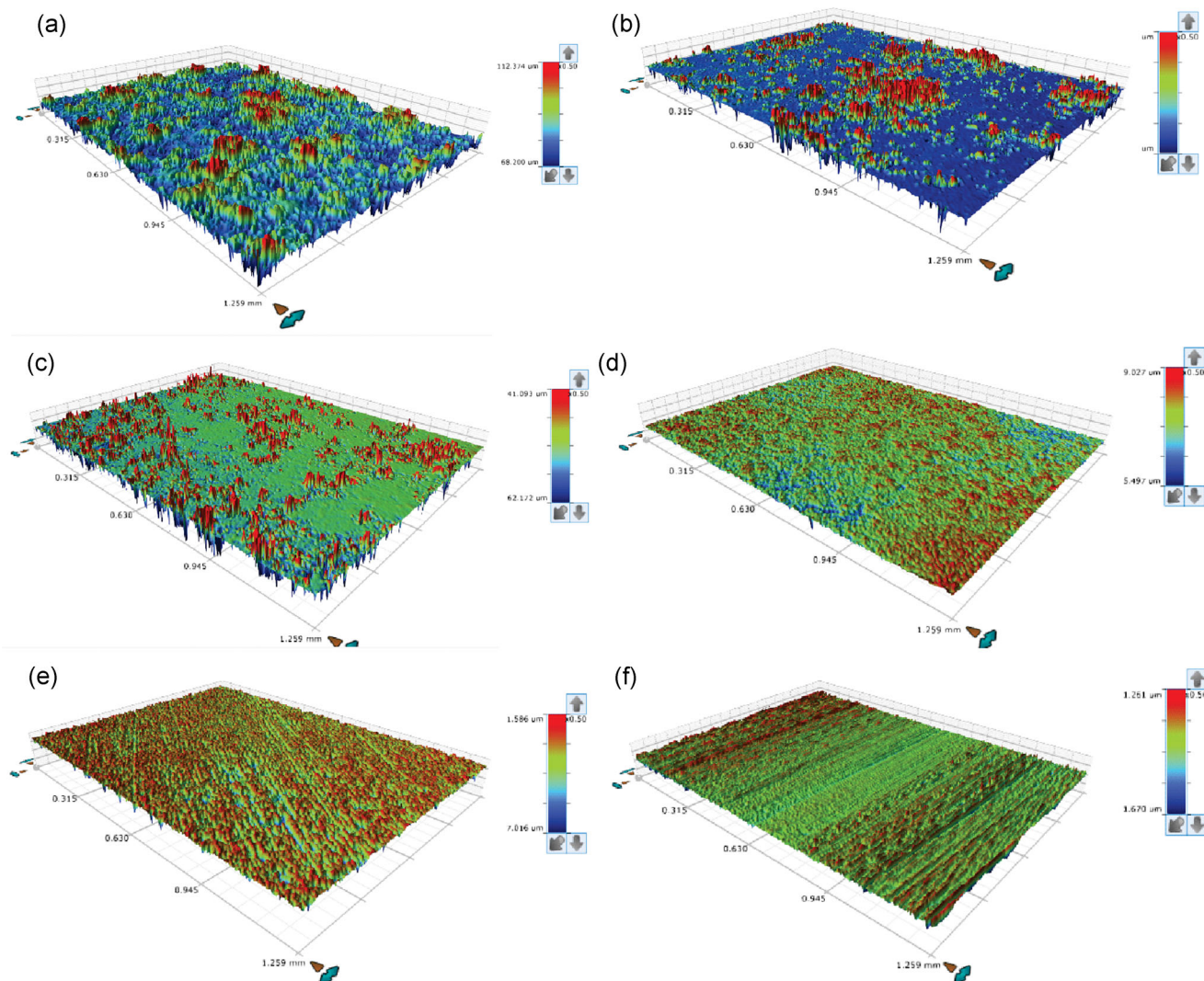

FIGURE 9 Topography evaluated by optical interferometry after 120-hr immersion in (a) 0.1-mol/L hydrochloric acid; (b) 0.25-mmol/L *N*-methyl-2-hydroxyethylammonium oleate ([m-2HEA][Ol]) + 0.1-mol/L hydrochloric acid; (c) 0.50-mmol/L [m-2HEA][Ol] + 0.1 mol/L hydrochloric acid; (d) 1.25-mmol/L [m-2HEA][Ol] + 0.1-mol/L hydrochloric acid; (e) 2.50-mmol/L [m-2HEA][Ol] + 0.1-mol/L hydrochloric acid; (f) clean steel [Color figure can be viewed at wileyonlinelibrary.com]

completely prevent corrosion attack. However, the presence of carbon and nitrogen in corrosion products indicates that the IL is able to react with iron by forming complexes that reduce the CR. Furthermore, chloride is detected, which makes the proposal of the aforementioned inhibition mechanism possible.

3D optical interferometry images are presented in Figure 9. The steel electrode after 120-hr immersion in 0.1-mol/L hydrochloric acid was strongly damaged, as evidenced by the increase of surface roughness (Figure 9a). Figure 9b–e presents the topography of samples in contact with [m-2HEA][Ol]-containing solutions, which reveals that the surface is not damaged, as it is possible to see preexistent grid marks. It is confirmed that corrosive attack was minimum when compared with clean steel (Figure 9f). In Figure 9b,c even with less general corrosion, some deep and localized attacks are observed. This aspect decreases with the increase in the inhibitor concentration.

Roughness (Sz) was obtained from optical interferometry (Figure 10), and it decreases with the increase of [m-2HEA][Ol] concentration, confirming that corrosion is strongly inhibited in PIL presence. With 2.5 mmol/L of [m-2HEA][Ol], the roughness was just a few points higher than for clean steel.

3.8 | Raman spectroscopy

Raman spectrum of the corrosion product of steel in contact with 0.1-mol/L hydrochloric acid appears in Figure 11. Characteristic bands corresponding to a mixture of iron oxides and hydroxides can be found in the corrosion product like lepidocrocite (γ-FeO(OH); 1,363, 273, 503 cm^{-1}), magnetite (Fe_3O_4; 700 cm^{-1}), and hematite (Fe_2O_3; 1,363, 231, 249, and 398 cm^{-1}).[88–90]

Figure 12a corresponds to Raman spectra obtained for samples immersed in an inhibited hydrochloric acid solution. In the images, the samples present both attacked and nonattacked zones. Spectra were acquired for both places to evaluate the chemical and structural differences between them. Black lines are spectra obtained directly on the corrosion products. For all samples in inhibited media, the corrosion product spectra indicate hematite (1,311, 397, 285, 216 cm^{-1}) and goethite (α-FeOOH; 595, 470 cm^{-1}) Raman shifts.[88,91,92] The presence of chlorinated, oxyhydroxide akaganeite (β-FeOOH) is also possible within the corrosion products, but its Raman shift can be masked by those of hematite and goethite; thus, this structure cannot be identified with precision.

The sample in contact with 2.5-mmol/L [m-2HEA][Ol] solution (Figure 12d) presents, on the corroded region, Raman shifts that belong to [m-2HEA][Ol]. It can
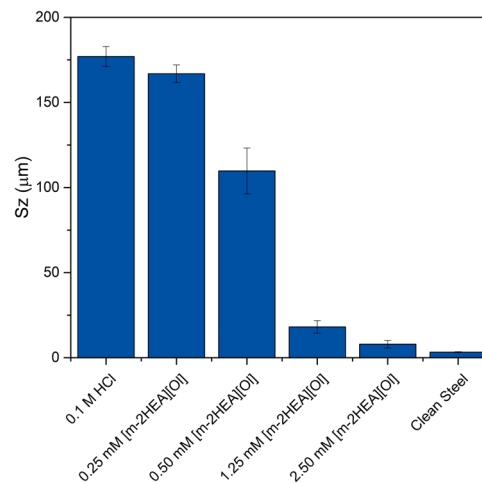

FIGURE 10　Roughness (Sz) of steel evaluated after 120-hr immersion for all studied systems, compared with polished steel. [m-2HEA][Ol], *N*-methyl-2-hydroxyethylammonium oleate [Color figure can be viewed at wileyonlinelibrary.com]

be attributed to a complex formed by the PIL and iron oxides and hydroxides.

However, spectra for the uncorroded regions (red lines in Figure 12c,d) display less definition of the bands of iron oxides/hydroxides and show the Raman shifts of the PIL 2,800–3,000, 1,433, 1,291, 1,080 cm^{-1}. This mitigated formation of iron oxide–hydroxide is caused by the blocking effect of the inhibitor, which is supported by polarization curves. In addition, as reported by Schmitzhaus et al.,[36] the PIL is able to form complexes with iron. It may promote the growth of the PIL adsorbed layer, as found by other authors for different inhibitors.[7,60,63,93] These characteristic Raman shifts of the
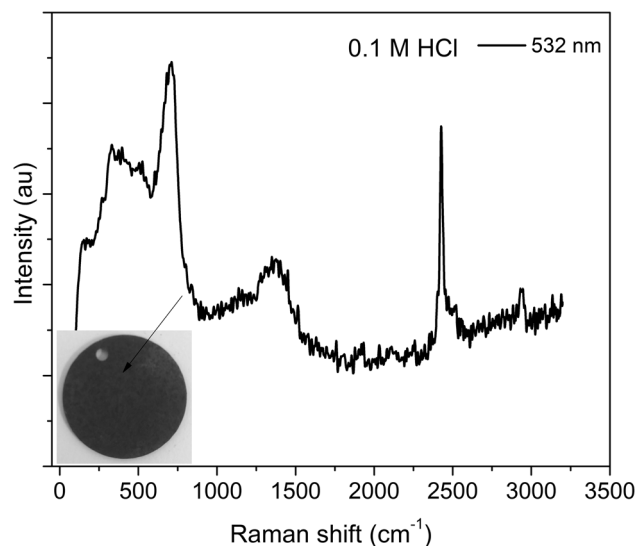

FIGURE 11　Raman spectrum for the corrosion product of steel in contact with 0.1-mol/L hydrochloric acid
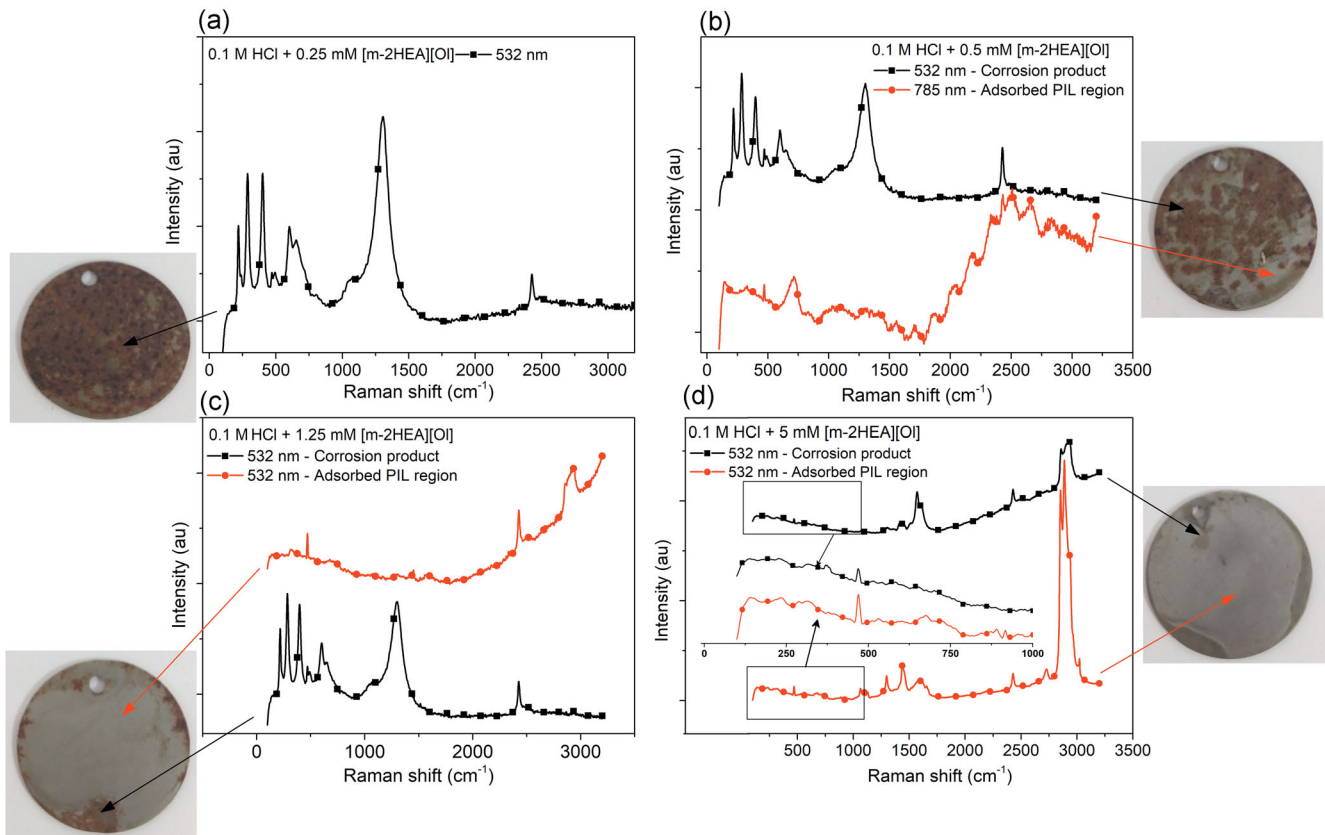
FIGURE 12 Raman spectrum for samples: (a) the corrosion product of steel in contact with 0.1-mol/L hydrochloric acid + 0.25-mmol/L *N*-methyl-2-hydroxyethylammonium oleate ([m-2HEA][Ol]); (b) the corrosion product of steel in contact with 0.1-mol/L hydrochloric acid + 0.5-mmol/L [m-2HEA][Ol]; (c) the corrosion product of steel in contact with 0.1-mol/L hydrochloric acid + 1.25-mmol/L [m-2HEA][Ol]; and (d) the corrosion product of steel in contact with 0.1-mol/L hydrochloric acid + 2.5-mmol/L [m-2HEA][Ol] [Color figure can be viewed at wileyonlinelibrary.com]
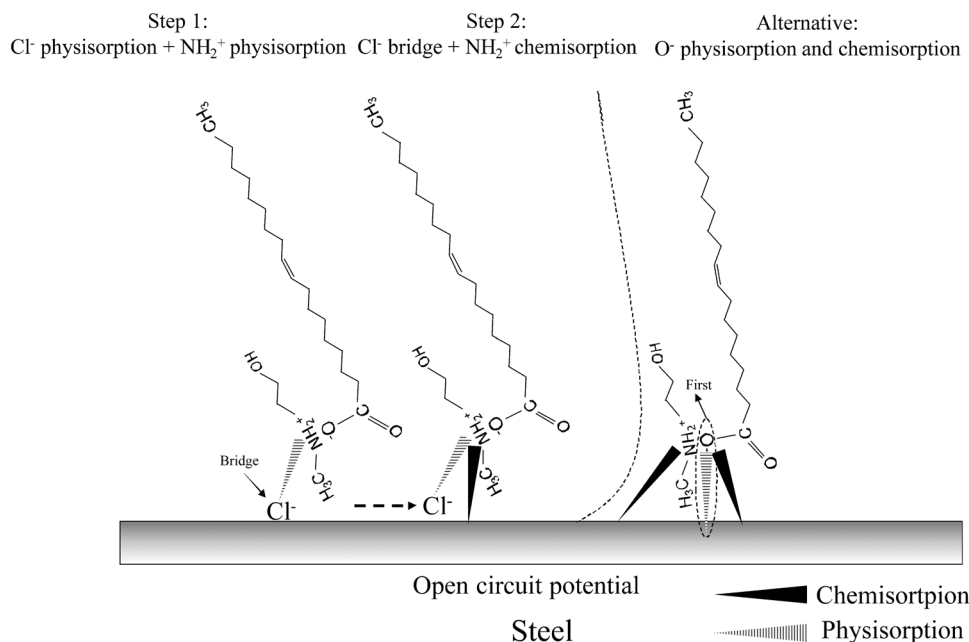

FIGURE 13 A schematic representation of the inhibiting mechanism proposed for *N*-methyl-2-hydroxyethylammonium oleate on the steel surface

PIL are stronger with the increase of the PIL concentration. PIL bands appear more definite in the 2.5-mmol/L spectrum than in the other ones. The surface coverage increases with the increase in the inhibitor concentration; in consequence, the substrate protection also increases along with the PIL Raman signal.

The activation energy reduction in the anodic branch of the polarization curve allows the fast formation of a corrosion product on which the PIL is adsorbed, as demonstrated by Raman spectra. The presence of both corrosion products (iron oxides and hydroxides) and PIL is observed. In consequence, despite reduction in β_a after PIL adsorption, there is also a decrease in the corrosion current density.

The presence of PIL at low concentration leads the anodic reaction to the preferential formation of hematite and goethite; meanwhile, hydrochloric acid medium yields a mixture of diverse iron oxides and hydroxides. At a higher PIL concentration, the same corrosion products observed for blank acid solutions are formed; however, they work out as support for PIL adsorption. The presence of this corrosion product can enhance the adsorption by both cation and anion moieties, whereas chloride ion acts as a bridge for the cation moiety adsorption.

Raman spectra corroborate that adsorption was strong enough, as the PIL could not be removed by washing. After the weight loss test, samples were washed with distilled and deionized water and dried with an air jet. However, the adsorbed layer kept itself stable and could not be removed by dissolution in water. This behavior was confirmed by wettability tests previously described, where the hydrophobic behavior was verified, thus explaining the stability of the adsorbed PIL layer against washing.

3.9 | Inhibition mechanism

A schematic diagram of the proposed corrosion inhibition mechanism of steel in 0.1-mol/L hydrochloric acid with the studied IL is presented in Figure 13. At OCP, which is above the E_{ZCP}, the net charge is positive and negative ions are expected to adsorb, such as chloride ions. After physical adsorption of chloride ion (Step 1 of Figure 13) on steel surface, NH_2^+ develops physisorption over Cl^- ion. It means that chloride ion acts as a bridge, i.e., it provides conditions for posteriori chemical adsorption of NH_2^+ group and/or O^- group (Step 2). But even if chloride ions are not present in solution, the O^- group has a physical attraction to the positive surface due to coulombic forces, and it may first adsorb physically and afterward share electron bonds, that is, chemisorption.

The long alkyl chain of the anionic part of PIL is able to block the diffusion of the most part of aggressive species.

Alvarez et al.[37] reported that due to the amphiphilic nature of these ILs, they have the ability to form lamellar structures. The hydrophobic alkyl chains of anion molecules would be packed together in the lamellar phase, leaving the polar carboxylate anion head exposed to the hydrophilic interlamellar space in close contact with the cation species.

The role of the double bond (unsaturation) in oleic part of PIL is believed to contribute to the efficiency, because the unsaturation can be adsorbed on the metal surface by a flat adsorption process, reducing the presence of active sites and blocking the corrosion process, as Schmitzhaus et al.[36] observed using the same IL in a nearly neutral solution. Porcayo-Calderon et al.[94] also reported the contribution of unsaturation in the alky chains of inhibitors to the efficiency in corrosion inhibition. The p-orbital of a double bond can interact with the vacant d-orbital of iron, and the metal surface can be covered by a dense and compact PIL film, which may prevent diffusion of corrosive species, thereby largely inhibiting corrosion.

3.10 | The role of chloride ion in corrosion inhibition

The effect of chloride ions on the inhibitive action of [m-2HEA][Ol] in a 0.1-mol/L hydrochloric acid solution was investigated by polarization curves. The aggressive environment was changed from 0.1-mol/L hydrochloric acid to 0.05-mol/L sulfuric acid, to isolate the action of chloride ion. Sodium chloride was added to the solution to obtain a chloride concentration of 0.1 mol/L, as in the studied hydrochloric acid solution. Furthermore, the inhibitor concentration was fixed at 2.5 mmol/L (the optimal concentration of [m-2HEA][Ol]). Polarization curves are shown in Figure 14 and the corrosion parameters are listed in Table 3.

It is well accepted that the presence of halide ions facilitates the adsorption of organic inhibitors by forming bridges between the cation moiety of the inhibitor and the metal surface.[95,96] An increase in inhibition efficiency could be observed in the presence of halide additives if protonated species of the inhibitor were utilized.[95]

Table 3 reveals that the solution containing 2.5-mmol/L [m-2HEA][Ol] achieves 93% of inhibition efficiency in a 0.1-mol/L hydrochloric acid solution and only 54% in a 0.05-mol/L sulfuric acid solution. This result is best explained in terms of adsorbability of Cl^- and SO_4^{2-}. The specific adsorption of anions is expected to be more pronounced with anions having a smaller degree of hydration, such as chloride ions.[97] Furthermore, a decrease of corrosion current is observed when chloride is added in a 0.05-mol/L sulfuric acid solution. As the
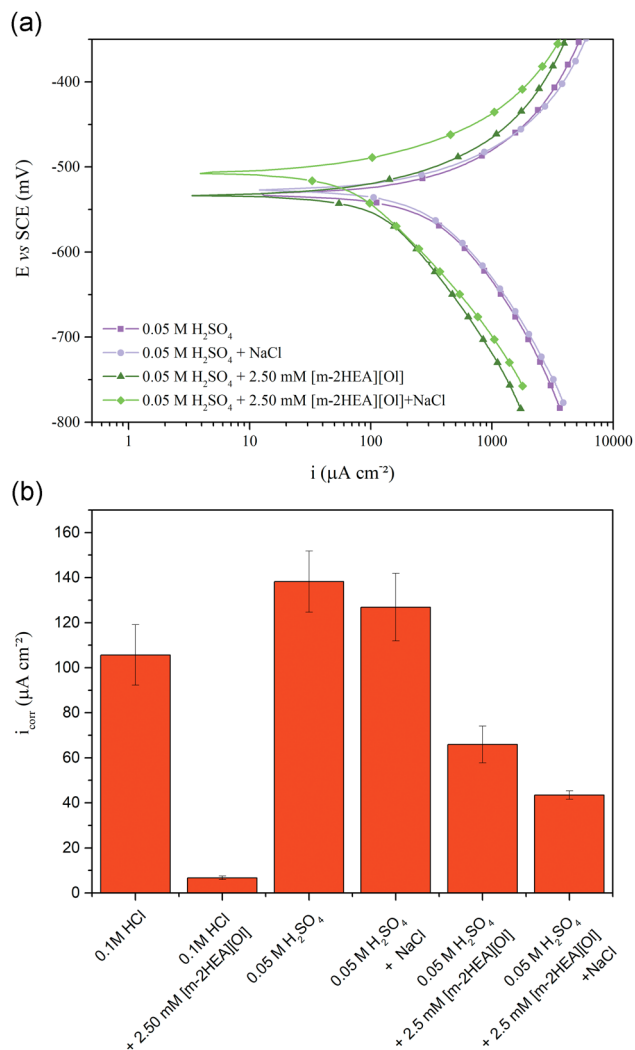
(a)

(b)

FIGURE 14 (a) Polarization curves in solutions containing 0.05-mol/L sulfuric acid, 2.5-mmol/L *N*-methyl-2-hydroxyethylammonium oleate ([m-2HEA][Ol]) and chloride; (b) a comparative chart of corrosion currents of steel in 0.1-mol/L hydrochloric acid, 0.1-mol/L hydrochloric acid + 2.5-mmol/L [m-2HEA][Ol], 0.05-mol/L sulfuric acid, 0.05-mol/L sulfuric acid + chloride, 0.05-mol/L sulfuric acid + 2.5-mmol/L [m-2HEA] [OL], and 0.05-mol/L sulfuric acid + 2.5-mmol/L [m-2HEA] [Ol] + chloride [Color figure can be viewed at wileyonlinelibrary.com]

standard deviation was relatively high, it is not possible to confirm that chloride affects the corrosion current at this condition, as revealed by Figure 14b. The adsorption of ILs does not always occur through direct interaction with steel. In some cases, the adsorption occurs through the already adsorbed chloride or sulfate ions that interfere with the adsorbed IL.[98] The interference by sulfate ions leads to lower adsorption and consequently lower corrosion inhibition. In fact, the specific adsorption of anions is expected to be more pronounced with anions having a smaller degree of hydration, such as chloride ions. Being specifically adsorbed, they neutralize a part of

the positive charge carried by steel and favor adsorption of cation moiety of [m-2HEA][Ol], at the corrosion potential, leading to an improved inhibition.[99,100]

The solution containing 0.05-mol/L sulfuric acid + PIL + chloride exhibits lower corrosion current density values than those without chloride ions (0.05-mol/L sulfuric acid + PIL). Besides, the corrosion potential shifts toward positive values with chloride addition, as revealed by Figure 14. It implies that chloride ions have a synergistic effect on the corrosion inhibition of mild steel in 0.05-mol/L sulfuric acid,[101] which can be explained by the chemisorption of chloride ions on the steel surface.[102,103] The PIL may then be adsorbed by coulombic attraction on the mild steel,[102] which will help to fill the voids in the adsorbed [m-2HEA][Ol] film.[100] The stabilization of the adsorbed chloride ions with the inhibitor leads to a greater surface coverage and creates conditions to promote chemisorption so that the molecules are at suitable distances for electron sharing, thereby resulting in better inhibition performance.[104]

4 | CONCLUSIONS

1. [m-2HEA][Ol] worked out as a corrosion inhibitor for steel in 0.1-mol/L hydrochloric acid solutions, and the inhibition efficiencies were observed to be increasing with an increase in the concentration of [m-2HEA] [Ol], reaching 94% efficiency with 2.5 mmol/L of PIL.
2. The presence of [m-2HEA][Ol] modified wettability of the steel surface, which increased the contact angle value, leading to a more hydrophobic behavior, due to the adsorption of [m-2HEA][Ol] on the steel surface, thus increasing the inhibitory effects.
3. ZCP indicated a positive free charge on the steel surface for all studied concentrations, at OCP, and that negatively charged molecules have a preference in physical adsorption. E_{ZCP} revealed a decrease of C_{dl} in the presence of PIL, caused by PIL adsorption.
4. Chronoamperometric tests revealed that injection of [m-2HEA][Ol] strongly affected the corrosion process, and at both cathodic and anodic potentials, the PIL inhibited both electrochemical reactions in more than 95%.
5. SEM, EDX, and optical interferometry revealed the formation of a smooth surface on steel in the presence of [m-2HEA][Ol] due to [m-2HEA][Ol] adsorption.
6. Raman spectra confirmed the PIL adsorption on the steel surface. Even in the presence of iron oxides, PIL was present in the same area, acting in the blocking effect. The formation of hematite and goethite was preferred at a low inhibitor concentration. The protected, noncorroded regions were rich in [m-2HEA] [Ol], as confirmed by the Raman signal.

7. A brief study on sulfuric acid revealed that the inhibitor is capable to work with 54% of inhibition efficiency in the presence of 2.5-mmol/L [m-2HEA][Ol].

8. The IL molecule acted by blocking the cathodic and anodic surface sites and by modifying the activation energy of the anodic reaction. The inhibition mechanism proposes that chloride ions act as a bridge for a posteriori adsorption of PIL, but it was also found that PIL itself can adsorb directly on the steel due to its ionic characteristics in both anodic and cathodic conditions.

ORCID

Tobias E. Schmitzhaus (iD) http://orcid.org/0000-0002-3667-8580

REFERENCES

[1] A. L. Chong, J. I. Mardel, D. R. MacFarlane, M. Forsyth, A. E. Somers, *ACS Sustainable Chem. Eng.* **2016**, *4*, 1746.

[2] R. Touir, N. Dkhireche, M. Ebn Touhami, M. Lakhrissi, B. Lakhrissi, M. Sfaira, *Desalination* **2009**, *249*, 922.

[3] L.-B. Niu, K. Nakada, *Corros. Sci.* **2015**, *96*, 171.

[4] O. Olivares-Xometl, C. López-Aguilar, P. Herrastí-González, N. V. Likhanova, I. Lijanova, R. Martínez-Palou, J. A. Rivera-Márquez, *Ind. Eng. Chem. Res.* **2014**, *53*, 9534.

[5] E. McCafferty, *Introduction to Corrosion Science*, Springer-Verlag, New York, NY **2010**.

[6] Z. Belarbi, J. M. Dominguez Olivo, F. Farelas, M. Singer, D. Young, S. Nešić, *Corrosion* **2019**, *75*, 1246.

[7] C. Verma, E. E. Ebenso, M. A. Quraishi, *J. Mol. Liq.* **2017**, *233*, 403.

[8] S. M. Tawfik, *J. Mol. Liq.* **2016**, *216*, 624.

[9] Z. Tao, W. He, S. Wang, G. Zhou, *Ind. Eng. Chem. Res.* **2013**, *52*, 17891.

[10] M. A. Deyab, M. M. Osman, A. E. Elkholy, F. E.-T. Heakal, *RSC Adv.* **2017**, *7*, 45241.

[11] P. Arellanes-Lozada, O. Olivares-Xometl, N. V. Likhanova, I. V. Lijanova, J. R. Vargas-García, R. E. Hernández-Ramírez, *J. Mol. Liq.* **2018**, *265*, 151.

[12] S.-H. Yoo, Y.-W. Kim, K. Chung, N.-K. Kim, J.-S. Kim, *Ind. Eng. Chem. Res.* **2013**, *52*, 10880.

[13] S. Mattedi, P. J. Carvalho, J. A. P. Coutinho, V. H. Alvarez, M. Iglesias, *J. Supercrit. Fluids* **2011**, *56*, 224.

[14] M. Iglesias, R. Gonzalez-Olmos, I. Cota, F. Medina, *Chem. Eng. J.* **2010**, *162*, 802.

[15] D. F. Kennedy, C. J. Drummond, *J. Phys. Chem. B* **2009**, *113*, 5690.

[16] Z. Fei, T. J. Geldbach, D. Zhao, P. J. Dyson, *Chem. - Eur. J.* **2006**, *12*, 2122.

[17] T. Tsuda, C. L. Hussey, *Electrochem. Soc. Interface* **2007**, *16*, 42.

[18] M. R. O. Vega, K. Parise, L. B. Ramos, U. Boff, S. Mattedi, L. Schaeffer, C. F. Malfatti, M. R. O. Vega, K. Parise, L. B. Ramos, U. Boff, S. Mattedi, L. Schaeffer, C. F. Malfatti, *Mater. Res.* **2017**, *20*, 675.

[19] P. Wasserscheid, W. Keim, *Angew. Chem., Int. Ed.* **2000**, *39*, 3772.

[20] T. Welton, *Chem. Rev.* **1999**, *99*, 2071.

[21] M. Echeverría, F. J. Deive, M. A. Sanromán, A. Rodríguez, C. M. Abreu, C. A. Echeverría, *Corrosion* **2014**, *71*, 259.

[22] Z. Zhao, Y. Shao, T. Wang, D. Feng, W. Liu, *Corrosion* **2009**, *65*, 674.

[23] M. R. Ortega Vega, J. Ercolani, S. Mattedi, C. Aguzzoli, C. A. Ferreira, A. S. Rocha, C. F. Malfatti, *Ind. Eng. Chem. Res.* **2018**, *57*, 12386.

[24] T. Espinosa, J. Sanes, A.-E. Jiménez, M.-D. Bermúdez, *Wear* **2013**, *303*, 495.

[25] X. B. Chen, H. Y. Yang, T. B. Abbott, M. A. Easton, N. Birbilis, *Corrosion* **2012**, *68*, 518.

[26] R. L. Vekariya, *J. Mol. Liq.* **2017**, *227*, 44.

[27] D. R. MacFarlane, N. Tachikawa, M. Forsyth, J. M. Pringle, P. C. Howlett, G. D. Elliott, J. H. Davis, M. Watanabe, P. Simon, C. Austen Angell, *Energy Environ. Sci.* **2014**, *7*, 232.

[28] D. Tempel, P. Henderson, J. Brzozowski, *US Patent 20040206241A1* **2004**.

[29] B. Weyershausen, K. Lehmann, *Green Chem.* **2005**, *7*, 15.

[30] D. Tromans, J. C. Silva, *Corrosion* **1997**, *53*, 16.

[31] J. Kadokawa, *Ionic Liquids: New Aspects for the Future*, IntechOpen, Rijeka, Croatia **2013**.

[32] N. V. Plechkova, K. R. Seddon, *Chem. Soc. Rev.* **2008**, *37*, 123.

[33] M. C. Bubalo, K. Radošević, I. R. Redovniković, J. Halambek, V. G. Srček, *Ecotoxicol. Environ. Saf.* **2014**, *99*, 1.

[34] M. A. Amin, K. F. Khaled, S. A. Fadl-Allah, *Corros. Sci.* **2010**, *52*, 140.

[35] M. A. Amin, M. M. Ibrahim, *Corros. Sci.* **2011**, *53*, 873.

[36] T. Schmitzhaus, M. Ortega-Vega, R. Schroeder, I. L. Muller, S. M. Silva, C. Malfatti, *Mater. Corros.* **2020**, https://doi.org/10.1002/maco.201911347

[37] V. H. Álvarez, S. Mattedi, M. Martin-Pastor, M. Aznar, M. Iglesias, *Fluid Phase Equilib.* **2010**, *299*, 42.

[38] E. McCafferty, *J. Electrochem. Soc.* **1974**, *121*, 1007.

[39] Y. Zou, J. Wang, Y. Y. Zheng, *Corros. Sci.* **2011**, *53*, 208.

[40] ASTM G102-89, *Practice for Calculation of Corrosion Rates and Related Information from Electrochemical Measurements*, ASTM International, West Conshohocken, PA **2015**.

[41] T. Douadi, H. Hamani, D. Daoud, M. Al-Noaimi, S. Chafaa, *J. Taiwan Inst. Chem. Eng.* **2017**, *71*, 388.

[42] G. Moretti, F. Guidi, F. Fabris, *Corros. Sci.* **2013**, *76*, 206.

[43] H. H. Hassan, E. Abdelghani, M. A. Amin, *Electrochim. Acta* **2007**, *52*, 6359.

[44] V. Sivakumar, K. Velumani, S. Rameshkumar, V. Sivakumar, K. Velumani, S. Rameshkumar, *Mater. Res.* **2018**, *21*, 1.

[45] Y. Qiang, S. Zhang, B. Tan, S. Chen, *Corros. Sci.* **2018**, *133*, 6.

[46] H. Ashassi-Sorkhabi, M. Es'haghi, *Mater. Chem. Phys.* **2009**, *114*, 267.

[47] B. Xu, Y. Liu, X. Yin, W. Yang, Y. Chen, *Corros. Sci.* **2013**, *74*, 206.

[48] T. Fallavena, M. Antonow, R. S. Gonçalves, *Appl. Surf. Sci.* **2006**, *253*, 566.

[49] E.-S. M. Sherif, R. M. Erasmus, J. D. Comins, *Electrochim. Acta* **2010**, *55*, 3657.

[50] ASTM G31-72, *Standard Practice for Laboratory Immersion Corrosion Testing of Metals*, ASTM International, West Conshohocken, PA **2004**.

[51] ASTM G1-03(2017)e1, *Standard Practice for Preparing, Cleaning, and Evaluating Corrosion Test Specimens*, ASTM International, West Conshohocken, PA **2017**.

[52] Y. Guo, B. Xu, Y. Liu, W. Yang, X. Yin, Y. Chen, J. Le, Z. Chen, *J. Ind. Eng. Chem.* **2017**, *56*, 234.

[53] V. Pandarinathan, K. Lepková, S. I. Bailey, T. Becker, R. Gubner, *Ind. Eng. Chem. Res.* **2014**, *53*, 5858.

[54] I. B. Obot, A. Madhankumar, *Mater. Chem. Phys.* **2016**, *177*, 266.

[55] G. A. Schmitt, N. Stradmann, presented at 98028 NACE Conf. Paper, 1998.

[56] V. H. Álvarez, N. Dosil, R. Gonzalez-Cabaleiro, S. Mattedi, M. Martin-Pastor, M. Iglesias, J. M. Navaza, *J. Chem. Eng. Data* **2010**, *55*, 625.

[57] C. Li, *Ph.D. Thesis*, Ohio University, **2009**.

[58] H. Luo, Y. C. Guan, K. N. Han, *Corrosion* **1998**, *54*, 619.

[59] A. Y. Musa, A. A. H. Kadhum, A. B. Mohamad, M. S. Takriff, A. R. Daud, S. K. Kamarudin, *Corros. Sci.* **2010**, *52*, 526.

[60] F. S. Souza, A. Spinelli, *Corros. Sci.* **2009**, *51*, 642.

[61] Y. Guo, Z. Chen, Y. Zuo, Y. Chen, W. Yang, B. Xu, *J. Mol. Liq.* **2018**, *269*, 886.

[62] S. Baldelli, *Acc. Chem. Res.* **2008**, *41*, 421.

[63] P. Roberge, *Handbook of Corrosion Engineering*, McGraw-Hill Professional, New York, NY **1999**.

[64] N. F. Atta, A. M. Fekry, H. M. Hassaneen, *Int. J. Hydrogen Energy* **2011**, *36*, 6462.

[65] S. L. Granese, *Corrosion* **1988**, *44*, 322.

[66] J. M. West, *Electrodeposition and Corrosion Processes*, Van Nostrand Reinhold, London, UK **1970**.

[67] D. M. Dražić, Lj Vračar, V. J. Dražić, *Electrochim. Acta* **1994**, *39*, 1165.

[68] B. Jegdić, J. Popić, B. Bobić, M. Stevanović, *Zast. Mater.* **2016**, *57*, 205.

[69] G. A. Marsh, E. Schaschl, *J. Electrochem. Soc.* **1960**, *107*, 960.

[70] G. M. Florianovich, *Russ. J. Electrochem.* **2000**, *36*, 1037.

[71] M. Rohwerder, K. de Weldige, M. Stratmann, *J. Solid State Electrochem.* **1998**, *2*, 88.

[72] M. Rohwerder, M. Stratmann, *MRS Bull.* **1999**, *24*, 43.

[73] P. Marcus, *Corrosion Mechanisms in Theory and Practice*, 3rd ed., CRC Press, Boca Raton, FL **2011**.

[74] N. Eldakar, K. Nobe, *Corrosion* **1976**, *32*, 238.

[75] E. McCafferty, N. Hackerman, *J. Electrochem. Soc.* **1972**, *119*, 146.

[76] W. J. Lorenz, *Corros. Sci.* **1965**, *5*, 121.

[77] A. Khamis, M. M. Saleh, M. I. Awad, *Corros. Sci.* **2013**, *66*, 343.

[78] A. A. Abdul Azim, L. A. Shalaby, H. Abbas, *Corros. Sci.* **1974**, *14*, 21.

[79] L. Feng, S. Zhang, Y. Lu, B. Tan, S. Chen, L. Guo, *Appl. Surf. Sci.* **2019**, *483*, 901.

[80] A. E. Guerraf, A. Titi, K. Cherrak, N. Mechbal, M. E. Azzouzi, R. Touzani, B. Hammouti, H. Lgaz, *Surf. Interfaces* **2018**, *13*, 168.

[81] M. M. Saleh, M. G. Mahmoud, H. M. Abd El-Lateef, *Corros. Sci.* **2019**, *154*, 70.

[82] S. A. A. El, *J. Electrochem. Sci.* **2008**, *3*, 28.

[83] R. Solmaz, G. Kardaş, B. Yazıcı, M. Erbil, *Colloids Surf., A* **2008**, *312*, 7.

[84] A. Łukomska, J. Sobkowski, *J. Electroanal. Chem.* **2004**, *567*, 95.

[85] R. Solmaz, *Corros. Sci.* **2014**, *81*, 75.

[86] A. Döner, G. Kardaş, *Corros. Sci.* **2011**, *53*, 4223.

[87] R. Solmaz, *Corros. Sci.* **2014**, *79*, 169.

[88] L. Bellot-Gurlet, D. Neff, S. Réguer, J. Monnier, M. Saheb, P. Dillmann, *J. Nano Res.* **2009**, *8*, 147.

[89] H. P. Dias, E. V. Barros, C. M. S. Sad, E. R. Yapuchura, A. O. Gomes, R. Moura, F. E. Pinto, D. V. Domingos, G. M. F. V. Aquije, V. Lacerda Jr., W. Romão, H. P. Dias, E. V. Barros, C. M. S. Sad, E. R. Yapuchura, A. O. Gomes, R. Moura, F. E. Pinto, D. V. Domingos, G. M. F. V. Aquije, V. Lacerda Jr., W. Romão, *J. Braz. Chem. Soc.* **2018**, *29*, 1690.

[90] J. Heuer, A. Luttge, *npj Mater. Degrad.* **2018**, *2*, 40.

[91] J. W. Anthony, *Handbook of Mineralogy*, Mineral Data Publishing, CA **1995**.

[92] Goethite X050091—RRUFF Database: Raman, X-ray, Infrared, and Chemistry, http://rruff.info/goethite/display=default/X050091 (accessed: September 2019).

[93] N. V. Likhanova, M. A. Domínguez-Aguilar, O. Olivares-Xometl, N. Nava-Entzana, E. Arce, H. Dorantes, *Corros. Sci.* **2010**, *52*, 2088.

[94] J. Porcayo-Calderon, I. Regla, E. Vazquez-Velez, L. M. Martinez de la Escalera, J. Canto, M. Casales-Diaz, *J. Spectrosc.* **2015**, *2015*, 1.

[95] M. N. El-Haddad, A. S. Fouda, *Chem. Eng. Commun.* **2013**, *200*, 1366.

[96] E. E. Oguzie, *Corros. Sci.* **2008**, *50*, 2993.

[97] T. Murakawa, N. Hackerman, *Corros. Sci.* **1964**, *4*, 387.

[98] S. Rengamani, S. Muralidharan, M. Anbu Kulandainathan, *J. Appl. Electrochem.* **1994**, *24*, 355.

[99] M. Djellab, H. Bentrah, A. Chala, H. Taoui, *Mater. Corros.* **2019**, *70*, 149.

[100] J. O. Bockris, B. Yang, *J. Electrochem. Soc.* **1991**, *138*, 2237.

[101] U. M. Eduok, U. J. Etim, A. E. Akpakpan, S. A. Umoren, *Int. J. Adv. Sci. Techn. Res.* **2012**, *1*, 23.

[102] F. Bentiss, M. Lebrini, M. Traisnel, M. Lagrenée, *J. Appl. Electrochem.* **2009**, *39*, 1399.

[103] R. T. Foley, *Corrosion* **1970**, *26*, 58.

[104] A. Y. Musa, A. B. Mohamad, A. A. H. Kadhum, M. S. Takriff, L. T. Tien, *Corros. Sci.* **2011**, *53*, 3672.

[105] C. Zuriaga-Monroy, R. Oviedo-Roa, L. E. Montiel-Sánchez, A. Vega-Paz, J. Marín-Cruz, J.-M. Martínez-Magadán, *Ind. Eng. Chem. Res.* **2016**, *55*, 3506.

[106] L. C. Murulana, A. K. Singh, S. K. Shukla, M. M. Kabanda, E. E. Ebenso, *Ind. Eng. Chem. Res.* **2012**, *51*, 13282.

[107] W. Villamizar, M. Casales, J. G. Gonzales-Rodriguez, L. Martinez, *Mater. Corros.* **2006**, *57*, 696.